

THE ISOTOPIC COMPOSITION OF COSMIC-RAY B, C, N, AND O: EVIDENCE FOR AN OVERABUNDANCE OF ^{18}O

P. S. GIBNER, R. A. MEWALDT, S. M. SCHINDLER, AND E. C. STONE
 220-47 Downs Laboratory, California Institute of Technology, Pasadena, CA 91125

AND

W. R. WEBBER

Department of Astronomy, Box 30001, Department 4500, New Mexico State University, Las Cruces, NM 88003

Received 1992 January 13; accepted 1992 March 12

ABSTRACT

New observations of galactic cosmic rays at higher energies ($\sim 400\text{--}780$ MeV nucleon $^{-1}$) than obtained in previous direct mass measurements have resulted in determinations of the isotopic composition of B, C, N, and O. The derived cosmic-ray source abundances provide evidence for an enhancement of $^{18}\text{O}/^{16}\text{O}$ by a factor of 5.6 ± 1.9 over the solar system value and give a $^{13}\text{C}/^{12}\text{C}$ ratio consistent with the solar system abundance ratio, but lower than some recent measurements of the local interstellar medium.

Subject headings: cosmic rays — Galaxy: abundances

1. INTRODUCTION

The isotopes of carbon, nitrogen, and oxygen are of interest due to their role in stellar nucleosynthesis and galactic chemical evolution. Optical and radio measurements of interstellar isotope abundances indicate significant differences from solar system abundances. Radio observations have measured an $^{17}\text{O}/^{18}\text{O}$ ratio in interstellar clouds of ~ 1.5 times the solar system ratio and have found possible evidence for an enhanced $^{18}\text{O}/^{16}\text{O}$ ratio at the Galactic center (Wannier 1985). Optical observations of five nearby molecular clouds (Hawkins & Jura 1987) find $^{13}\text{C}/^{12}\text{C} = 0.023 \pm 0.003$, as compared to the solar system value of 0.011. Two more recent optical observations of CH^+ (Stahl & Wilson 1991; Crane, Hegyi, & Lambert 1991) resulted in $^{13}\text{C}/^{12}\text{C}$ values of 0.014 ± 0.001 and 0.015 ± 0.001 .

Langer & Penzias' (1990) millimeter-wave observations of CO result in a $^{13}\text{C}/^{12}\text{C}$ ratio ranging from 0.014 at a Galactic radius of 12 kpc to about 0.033 at 5 kpc, with a ratio at the Galactic center of 0.042. Their $^{13}\text{C}/^{12}\text{C}$ value of 0.018 near the solar radius falls between the optical CH^+ measurements. Note that some galactic chemical evolution models predict that the $^{13}\text{C}/^{12}\text{C}$ ratio in the ISM should have increased since the time of solar system formation (see, e.g., Audouze 1985; Tosi 1988).

The composition of cosmic-ray source (CRS) material has been shown to be similar to that of the solar system, with some significant differences which indicate that their nucleosynthetic history has differed. Enhanced abundances of the neutron-rich isotopes ^{22}Ne , ^{25}Mg , and ^{26}Mg have been found in cosmic rays (see, e.g., the review in Mewaldt 1989), and there is possible evidence for enhanced ^{29}Si and ^{30}Si abundances as well (Wiedenbeck & Greiner 1991a; however, see Webber et al. 1990e).

CRS abundances of C, N, and O show a C/O ratio that is about twice the solar system value and a N/O ratio at least 3 times smaller than in the solar system. While these elemental abundance anomalies suggest that isotopic differences might be expected as well, determinations of the CRS isotopic composition are hampered by the relatively large contributions of ^{13}C , ^{17}O , and ^{18}O produced during cosmic-ray propagation in

the ISM. As a result, it has been difficult to establish whether the CRS and solar system abundances of C, N, or O isotopes differ (see, e.g., Wiedenbeck & Greiner 1981a, b; Gupta & Webber 1989; and the review in Mewaldt 1989). In this *Letter* we report new measurements of cosmic-ray B, C, N, and O isotopes at higher energies than previous direct mass measurements and derive CRS abundances using an interstellar propagation model that includes improved fragmentation cross sections. We present evidence for a significant overabundance of ^{18}O in CRS material.

2. OBSERVATIONS

Observations reported here were made with the Caltech balloon-borne High Energy Isotope Spectrometer Telescope (HEIST) during a flight on 1988 August 25–27 from Prince Albert, Saskatchewan. Figure 1 shows the main detector elements of HEIST, including its stack of 12 NaI(Tl) scintillators (Schindler et al. 1983), each nominally 2 cm thick and 52 cm in diameter, which are used to measure the total energy of stopping nuclei. Particle trajectories through the instrument are determined by analyzing the distribution of scintillation light among the six photomultiplier tubes viewing each NaI(Tl) layer. The resulting position accuracy is ~ 4 mm in each layer for the nuclei of interest here. The velocity of incident nuclei is measured by the Cerenkov counters C1, which contains a Teflon radiator, and C2, which has a Pilot-425 radiator (Christian et al. 1987). The index of refraction of C1, $n = 1.36$, corresponds to a threshold energy of 442 MeV nucleon $^{-1}$, while C2's index of refraction, $n = 1.52$, has a threshold of 305 MeV nucleon $^{-1}$. The plastic scintillator, S1, provides an event trigger and an energy loss (ΔE) measurement used for charge identification, while scintillator S2 identifies events penetrating the entire stack.

For each event analyzed, HEIST provides three separate charge measurements and either two or three separate mass measurements. Two charge measurements are based on the Cerenkov versus dE/dx technique using energy deposition measurements in S1 and in NaI(Tl) layer L1, combined with the C2 response. The final charge measurement is based on the

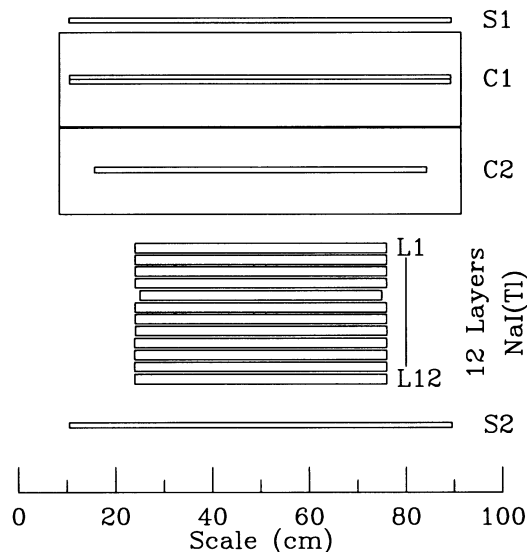


FIG. 1.—A cross section of HEIST including scintillators S1 and S2, Cerenkov counters C1 and C2, and NaI(Tl) scintillator layers L1 to L12.

energy losses in the layers of the NaI(Tl) stack. Consistency requirements between the three charge measurements identify events which undergo nuclear interactions within the system and other “background” events.

Only events which stop within the NaI(Tl) stack are candidates for mass analysis. By combining either the C1 or C2 response with the total energy deposition in the NaI(Tl) stack, the mass can be determined using the Cerenkov–total energy method. In addition, for all analyzed events the mass can be measured by the energy loss (ΔE) versus residual energy (E') technique using energy losses in the NaI(Tl) stack. Thus HEIST provides two mass measurements for events with velocities above C2 threshold but below C1 threshold, and three mass measurements for events which are above both Cerenkov thresholds. Combining these mass measurements results in better mass resolution than from any single measurement, and consistency cross-checks further reduce background.

The mass distributions for each element were fitted using the maximum likelihood method to determine isotopic abundances. Mass histograms for B, C, N, and O, constructed by finding the weighted average of the mass estimators for each

event, are shown in Figure 2. The rms mass resolution varies from ~ 0.24 amu at boron to ~ 0.27 amu at oxygen. Nuclear interactions of cosmic rays during propagation through the atmosphere produce small abundances of the radioactive isotopes ^{10}C , ^{11}C , ^{14}C , ^{13}N , ^{16}N , ^{14}O , and ^{15}O visible in Figure 2. Top-of-instrument abundances were found by correcting for events which had been rejected because they fragmented in the instrument and for small differences in the energy interval accepted for each isotope of a given element. To find top-of-atmosphere abundances corresponding to the observed abundances at HEIST's mean altitude of 5.15 g cm^{-2} of residual atmosphere, propagation through the atmosphere was modeled for isotopes of elements in the range $Z = 5\text{--}26$. For these calculations, nuclear interaction cross sections were extrapolated from measurements of various species incident on carbon targets (Webber, Kish, & Schrier, 1990a, b, c). We have used experimentally determined cross sections where available and a modified empirical model (by one of us [W. W.]) for unmeasured cross sections. Comparing the predicted and observed numbers for each of the radioactive isotopes gives a reduced χ^2 value of 1.17, with 7 degrees of freedom, so the model predictions agree reasonably well with the observed number of events. Resulting abundances, extrapolated to the top of the atmosphere, are shown in Table 1.

3. INTERPRETATION

To relate our observations at 1 AU to abundances at the CRS, we used a “leaky-box” propagation model in which all species are assumed to have a common source spectrum with $dJ/dE \propto P^{-2.3}$ where P is momentum, and a rigidity-dependent path length given by $\lambda_e = 42.4\beta^{3/2}R^{-0.65} \text{ g cm}^{-2}$ for rigidities (R) above 3.7 GV, and $\lambda_e = 18.1\beta^{3/2} \text{ g cm}^{-2}$ for lower rigidities, where β is the ratio of the particle velocity to the velocity of light. The model includes the effects of nuclear fragmentation and ionization energy losses in interstellar H and He, assuming 16% ionized H and $\text{He}/\text{H} = 0.07$, and new fragmentation cross section data from Webber et al. (1990a, b, c). Unmeasured cross sections were calculated from the new empirical formulation of Webber, Kish, & Schrier (1990d). CRS elemental abundances have been taken from Engelmann et al. (1990), except that nitrogen has been adjusted such that $\text{N}/\text{O} = 0.04$. Solar modulation was accounted for using a spherically symmetric model (Fisk 1971) with a modulation

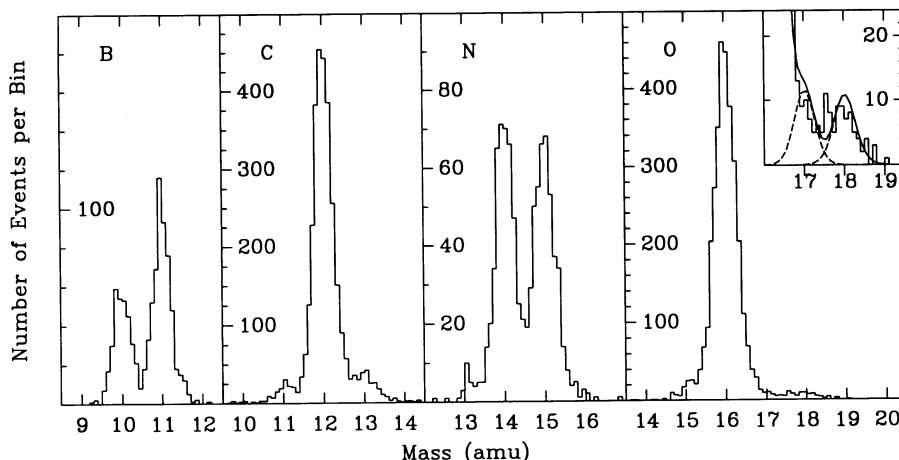


FIG. 2.—Mass histograms of B, C, N, and O nuclei. The rms mass resolution varies from ~ 0.24 amu at boron to ~ 0.27 amu at oxygen. An inset with an expanded scale shows the mass distribution fits for ^{17}O and ^{18}O .

TABLE 1
ISOTOPIC ABUNDANCE RATIOS

Isotope Ratio	Energy (MeV nucleon $^{-1}$)	Events Observed	Top of Instrument ^a	Top of Atmosphere ^b	CRS ^c	Average CRS ^{c,d}	Solar System ^e
$^{10}\text{B}/\text{B}$	414–640	327/889	0.305 ± 0.015	0.285 ± 0.016
$^{15}\text{N}/\text{N}$	446–681	447/879	0.533 ± 0.019	0.541 ± 0.025	0.0037
$^{13}\text{C}/^{12}\text{C}$	431–674	257/2686	0.103 ± 0.008	0.089 ± 0.008	$0.005^{+0.011}_{-0.005}$	0.004 ± 0.010	0.0112
$^{17}\text{O}/^{16}\text{O}$	463–777	77/3026	0.024 ± 0.006	0.019 ± 0.006	<0.007	0.0026 ± 0.0030	0.0004
$^{18}\text{O}/^{16}\text{O}$	463–777	71/3026	0.02778 ± 0.0033	0.0273 ± 0.0033	0.0115 ± 0.0038	0.0075 ± 0.0024	0.0020

^a Normalized to equal energy intervals. The 68% confidence limits include uncertainties from counting statistics, fitting, and instrument fragmentation corrections.

^b Estimated uncertainties from atmospheric corrections included in 68% confidence limits.

^c Includes propagation uncertainties assuming 10% uncorrelated errors in the measured cross sections and 20% uncorrelated errors for cross sections from the empirical formula.

^d A weighted average of the CRS abundances derived from the measurements in Fig. 3.

^e Cameron 1982.

level of $\phi = 650$ MV, as required to fit the oxygen spectrum of Engelmann et al. (1990). The mean path length was fitted to the B/C measurements at low energies by Krombel & Wiedenbeck (1988), and at higher energies by Engelmann et al. (1990), since the solar modulation level at the time of their measurements was comparable to that during our flight. Fitting the B/C ratio with other source spectra and path-length distributions combined with appropriate modulation levels from 500 to 800 MV shows that the B, C, N, and O isotopic composition is insensitive to the specific combination of source spectra, path length, and modulation level used, given the constraint of fitting the B/C measurements and the ^{16}O spectrum.

The model also agrees well with the observed F/Ne ratio (Engelmann et al. 1990) indicating that it accurately accounts for production of lighter fragments from Ne, Mg, and Si. Figure 3 compares our measurements with selected satellite and balloon observations, along with results from the propagation model. Table 1 lists derived abundances at 1 AU and at the CRS. Estimated propagation uncertainties have been included in the CRS error bars by assuming 10% uncorrelated uncertainties in the cross sections measured by Webber et al., and 20% uncorrelated uncertainties in the cross sections estimated from Webber's empirical model.

4. DISCUSSION

Essentially all of the boron observed in cosmic rays is believed to be of "secondary" origin, produced by fragmentation of heavier "primary" cosmic rays as they pass through interstellar material. The agreement of the $^{10}\text{B}/\text{B}$ observations with the propagation model therefore serves as a check on the model and cross sections. Most cosmic-ray N is also of secondary origin. Our observations of $^{14}\text{N}/\text{O}$ and $^{15}\text{N}/\text{O}$ lead to a CRS value of $^{14}\text{N}/\text{O} = 0.040 \pm 0.014$, ~ 3 –4 times smaller than in the solar system, and $^{15}\text{N}/\text{O} \leq 0.04$, favoring no ^{15}N in CRS material. These nitrogen results are consistent with a number of earlier studies including Krombel & Wiedenbeck (1988) and Gupta & Webber (1989).

Our $^{13}\text{C}/^{12}\text{C}$ measurement favors a CRS ^{13}C abundance that is lower than that in the solar system, as do all the measurements in Figure 3 and a recent *Voyager* measurement at 22 AU (Lukasiak et al. 1991). However, taking into account the uncertainty in the production of secondary ^{13}C , our $^{13}\text{C}/^{12}\text{C}$ measurement is consistent with either a solar system ^{13}C abundance or with no ^{13}C in the CRS. Taking a weighted average of the measurements in Figure 3 we find $^{13}\text{C}/^{12}\text{C} = 0.004 \pm 0.010$ at the CRS, including propagation uncertainties. This result is

slightly below the solar system value and 1σ below the Stahl & Wilson (1991) level of ^{13}C in the ISM; however, it is 1.9σ below the Hawkins & Jura (1987) $^{13}\text{C}/^{12}\text{C}$ ISM value. Webber & Soutoul (1989) also concluded that the CRS $^{13}\text{C}/^{12}\text{C}$ ratio is below the Hawkins & Jura measurement. With the present

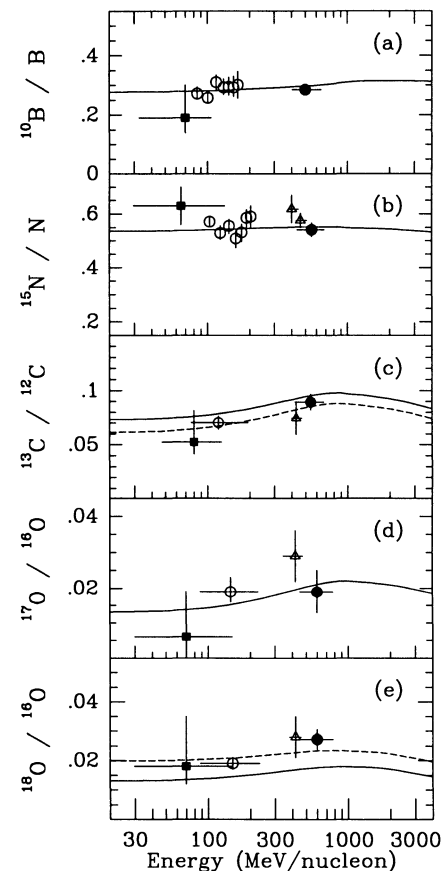


FIG. 3.—Comparison of cosmic-ray isotope measurements having mass resolution of 0.3 amu or better. The solid curves show the results of propagation calculations which assume solar system isotopic abundances at the cosmic-ray source. The dashed curve of panel (c) assumes zero abundance of ^{13}C at the source, and the dashed curve of panel (e) results from an $^{18}\text{O}/^{16}\text{O}$ ratio of 0.0075 at the source. Measurements: filled circle: this work; open circles: Krombel & Wiedenbeck (1988), Wiedenbeck & Greiner (1981a, b); filled squares: Mewaldt et al. (1981); triangles: Webber et al. (1985), Webber (1982). Summaries of additional isotope measurements can be found in Wiedenbeck (1984) and Mewaldt (1989).

uncertainties on the CRS and ISM measurements it is not possible to tell if these two samples of matter have different $^{13}\text{C}/^{12}\text{C}$ ratios.

Our measured source abundance of ^{17}O is consistent with the near-zero solar system ^{17}O abundance; however, the derived ^{18}O abundance at the CRS indicates an enrichment of ^{18}O relative to the solar system ratio of $^{18}\text{O}/^{16}\text{O} = 0.0020$ by a factor of 4–8. This ^{18}O overabundance cannot be due to uncertainties in the atmospheric corrections because we find that only $\sim 5\%$ of the observed ^{18}O is produced in the atmosphere. A CRS excess of ^{18}O is also indicated by all of the other measurements in Figure 3, when interpreted using our propagation model, and by the results of Lukasiak et al. (1991). Taking a weighted average of the measurements in Figure 3e results in a CRS value of $^{18}\text{O}/^{16}\text{O} = 0.0075 \pm 0.0024$, 2.3σ above the solar system value, including propagation uncertainties.

The conclusion that the CRS $^{18}\text{O}/^{16}\text{O}$ ratio derived from this and previous experiments exceeds the solar system value would not be possible without recent improvements in our knowledge of the fragmentation cross sections. The new cross section measurements and formulae have smaller uncertainties than cross section estimates employed earlier, and they predict a somewhat smaller secondary contribution to ^{18}O . Approximately 53% of the secondary ^{18}O comes from primaries which have measured fragmentation cross sections. The partial cross sections used in our propagation model would have to be changed by $\sim 34\%$ (correlated changes) to 70% (uncorrelated changes), in order to produce the weighted average $^{18}\text{O}/^{16}\text{O}$ ratio given a source with solar composition.

This study has used a source spectrum $dJ/dE \propto P^{-2.3}$, common to a number of earlier studies (e.g., Engelmann et al. 1990). Use of a pure rigidity power law, $dJ/dR \propto R^{-2.3}$, would increase the derived CRS $^{18}\text{O}/^{16}\text{O}$ ratio by $\sim 15\%$, with somewhat smaller increases for the other neutron-rich species in Table 1. Use of this latter source spectrum should be considered because it appears to be consistent with the predictions of some shock acceleration models (see, e.g., Blandford & Eichler 1987).

Various models have been proposed to explain the Ne, Mg, and Si isotope anomalies in cosmic rays. The “super-metallicity” model (Woosley & Weaver 1981) in which cosmic rays originate from metal-rich regions of the Galaxy predicts roughly equal enhancements for ^{18}O , ^{22}Ne , ^{25}Mg , ^{26}Mg , ^{29}Si , ^{30}Si , and other neutron-rich nuclei. If normalized to fit the Mg isotope abundances, the model falls short of explaining the

observed factor of 4–7 excess of ^{22}Ne in cosmic rays (Mewaldt 1989), and predicts a relatively weak ($\sim 50\%$) excess of ^{18}O . If normalized to fit ^{22}Ne and ^{18}O , it would predict enhancements for the neutron-rich Mg and Si isotopes that are larger than observed.

The Wolf-Rayet (WR) model (Cassé & Paul 1982; Prantzos, Arnould, & Arcoragi 1987), in which a fraction of the cosmic rays originate from material expelled by Wolf-Rayet stars, predicts enhancements in ^{12}C , ^{16}O , ^{22}Ne , ^{25}Mg , and ^{26}Mg . The model predicts that the CRS ratio for $^{13}\text{C}/^{12}\text{C}$ should be lower than in the solar system, but the resulting $^{18}\text{O}/^{16}\text{O}$ ratio is still in question. Simulations of WR star evolution do indicate a large ^{18}O excess during the first few thousand years of core He burning (Prantzos et al. 1986), but the short lifetime of this excess limits the amount of ^{18}O expelled (see also Langer 1991). For WR stars of 15 solar masses, Cassé & Paul (1982) predict an enhancement of $^{18}\text{O}/^{16}\text{O}$ by a factor 2.5 over the solar system value; however, it appears that more massive WR stars would not produce an enhancement of this size (Meyer 1985; Prantzos et al. 1986).

Olive & Schramm (1982) suggested that cosmic rays may be representative of the ISM composition and that the solar system may have formed as part of an OB association and have been enriched by the ejecta of supernovae within the association. The resulting “anomalous” solar system would be enriched in α -particle nuclei such as ^{12}C , ^{16}O , and ^{20}Ne . Normalizing to this “anomalous” solar system composition, the model predicts that both the ISM and cosmic rays will show enhancements in C/O, ^{22}Ne , ^{17}O , ^{18}O , and ^{13}C , qualitatively consistent with the observations except that we find no evidence for a ^{13}C excess in the cosmic rays.

In summary, the new $^{18}\text{O}/^{16}\text{O}$ observations presented here provide additional evidence for differences between the isotopic composition of cosmic-ray and solar system material. While current observations appear to favor the Wolf-Rayet model, it is not clear that any of the presently available models for cosmic-ray origin accounts quantitatively for all of these observed differences.

This work was supported in part by NASA under grant NAGW-1919. We thank A. Buffington, D. Burke, E. Christian, J. Grove, I. Rasmussen, J. Weger, and the Caltech Central Engineering Services for their contributions to HEIST and the National Scientific Balloon Facility and NASA Wallops Flight Facility for their excellent support.

REFERENCES

- Audouze, J. 1985, in *Production and Distribution of C, N, O Elements*, ed. I. J. Danziger, F. Matteucci, & K. Kjar (Munich: ESO), 373
- Blandford, R., & Eichler, D. 1987, *Phys. Rep.*, 154, 1
- Cameron, A. G. W. 1982, in *Essays in Astrophysics*, ed. C. A. Barnes, D. O. Clayton, & D. N. Schramm (Cambridge: Cambridge Univ. Press), 23
- Cassé, M., & Paul, J. A. 1982, *ApJ*, 258, 860
- Christian, E. R., Grove, J. E., Mewaldt, R. A., Schindler, S. M., Zukowski, T., Kish, J. C., & Webber, W. R. 1987, *Proc. 20th Internat. Cosmic Ray Conf. (Moscow)*, 2, 382
- Crane, P., Hegyi, D. J., & Lambert, D. L. 1991, *ApJ*, 378, 181
- Engelmann, J. J., et al. 1990, *A&A*, 233, 96
- Fisk, L. A. 1971, *J. Geophys. Res.*, 76, 221
- Gupta, M., & Webber, W. R. 1989, *ApJ*, 340, 1124
- Hawkins, I., & Jura, M. 1987, *ApJ*, 317, 926
- Krombel, K. E., & Wiedenbeck, M. E. 1988, *ApJ*, 328, 940
- Langer, N. 1991, *A&A*, 248, 531
- Langer, W. D., & Penzias, A. A. 1990, *ApJ*, 357, 477
- Lukasiak, A., Ferrando, P., McDonald, F. B., & Webber, W. R. 1991, *Proc. 22nd Internat. Cosmic Ray Conf. (Dublin)*, in press
- Mewaldt, R. A. 1989, in *AIP Conf. Proc. 183, Cosmic Abundances of Matter*, ed. C. J. Waddington (New York: AIP), 124
- Mewaldt, R. A., Spalding, J. D., Stone, E. C., & Vogt, R. E. 1981, *ApJ*, 251, L27
- Meyer, J.-P. 1985, *ApJS*, 57, 173
- Olive, K. A., & Schramm, D. N. 1982, *ApJ*, 257, 276
- Prantzos, N., Arnould, M., & Arcoragi, J.-P. 1987, *ApJ*, 315, 209
- Prantzos, N., Doom, C., Arnould, M., & de Loore, C. 1986, *ApJ*, 304, 695
- Schindler, S. M., Buffington, A., Lau, K., & Rasmussen, I. L. 1983, *Proc. 18th Internat. Cosmic Ray Conf. (Bangalore)*, 8, 73
- Stahl, O., & Wilson, T. L. 1991, preprint
- Tosi, M. 1988, *A&A*, 197, 33
- Wannier, P. G. 1985, in *Production and Distribution of C, N, O Elements*, ed. I. J. Danziger, F. Matteucci, & K. Kjar (Munich: ESO), 233
- Webber, W. R. 1982, *ApJ*, 252, 386
- . 1990, private communication
- Webber, W. R., Kish, J. C., & Schrier, D. A. 1985, *Proc. 19th Internat. Cosmic Ray Conf. (La Jolla)*, 2, 88
- . 1990a, *Phys. Rev. C*, 41, 520
- . 1990b, *Phys. Rev. C*, 41, 533
- . 1990c, *Phys. Rev. C*, 41, 547
- . 1990d, *Phys. Rev. C*, 41, 566
- Webber, W. R., & Soutoul, A. 1989, *A&A*, 215, 128
- Webber, W. R., Soutoul, A., Ferrando, P., & Gupta, M. 1990e, *ApJ*, 348, 611
- Wiedenbeck, M. E. 1984, *Adv. Space Res.*, 4, 15
- Wiedenbeck, M. E., & Greiner, D. E. 1981a, *ApJ*, 247, L119
- . 1981b, *Phys. Rev. Lett.*, 46, 682
- Woosley, S. E., & Weaver, T. A. 1981, *ApJ*, 243, 651